ELSEVIER

Ab initio calculations of the oxygen–vacancy dipoles and M centers in CaF$_2$

H. Shi *, R.I. Eglitis, G. Borstel

Fachbereich Physik, Universität Osnabrück, D-49069 Osnabrück, Germany

Abstract

We performed *ab initio* calculations of complex defects in CaF$_2$ namely oxygen–vacancy (OV) dipoles and F$_2$ centers (M centers) by means of the hybrid B3PW method, in which Hartree–Fock exchange is mixed with density functional theory (DFT) exchange functionals, using Becke's three parameter method, combined with the non-local correlation functionals by Perdew and Wang. Our calculated optical absorption bands for the OV center (6.40 eV, 6.52 eV and 6.66 eV) are in good agreement with the complex experimental 6.7 eV absorption bands consisting of at least two elementary peaks with separation of 0.48 eV. The defect levels induced by the oxygen impurity between the conduction and valence bands consist mainly of oxygen p orbitals and are split into three bands. Vacancy s orbitals form the vacancy band near the fermi-energy. Several configurations of the (OV)$_2$-dimer were calculated. The association energy for the most favorable one is 0.55 eV. The results for the M center, the simplest aggregation of two F centers, show that the β band absorption in CaF$_2$ is predominantly due to the presence of M centers. The direct optical gap for M centers in CaF$_2$ is 2.22 eV and is in good agreement with the corresponding experimental value of 2.38 eV.

1. Introduction

Considering the high technological importance of CaF$_2$, it is not surprising, that during the last years, it has been the subject of many experimental and theoretical studies [1–15]. Certain aspects of this research recently gained large interest in the context of the use of CaF$_2$ as an optical material for the deep ultraviolet (DUV) and vacuum ultraviolet (VUV) spectral regions.

Many alkali halides provide an attractive medium for color center research because of the ease with which they can be grown in reasonably pure single-crystal form and because they may be colored by ionizing radiations. Con-

temporary knowledge of defects in solids has helped to create a field of technology, namely, *defect engineering*, which is aimed at manipulating the nature and concentration of defects in a material so as to tune its properties in a desired manner to generate different behavior. CaF$_2$ could become an important optical material if one could avoid or, at least, control the photoinduced defect formation, which so far in applications degrades its optical quality. Therefore, it is important to understand the nature of defects in CaF$_2$.

Two kinds of intrinsic color center have been observed in CaF$_2$ by electron spin-resonance techniques. One is the V_k, or self-trapped hole, whose resonance has been reported by Hayes and Twidell [16] in X-rayed CaF$_2$ at liquid-nitrogen temperatures (LNT). The other is the F center, an electron trapped in an anion vacancy, whose resonance has been found by Arends [17] in additively colored

crystals and correlated with an optical absorption band at 3.3 eV.

On the other hand, one of the big unsolved problems in the context of the application of CaF_2 as an optical material is oxygen contamination in the bulk and at the surface. Oxygen is readily incorporated into the bulk during crystal growth and it is very difficult to avoid this contamination or to remove contaminants after growth. In the present paper, performing first principles calculations, we intend, firstly, to clarify the electronic structure, atomic geometry and band structure of OV dipoles and, secondly, to study the aggregation of the OV dipoles.

In a second part of paper, as an extension of our previous study dealing with the CaF_2 electronic structure and F centers therein [1], we also performed *ab initio* calculations of more complex defects in CaF_2, namely the F_2 center (or M center) which is composed of two F centers, by means of the hybrid B3PW method.

2. Method of calculations

We performed calculations for OV centers and M centers in CaF_2 using the hybrid B3PW method, which gives the best agreement with experiment for the lattice constant, bulk modulus and optical band gap [1]. The calculations were performed using the hybrid exchange-correlation B3PW functional involving a hybrid of non-local Fock exact exchange, local density approximation (LDA) exchange and Becke's gradient corrected exchange functional [18], combined with the nonlocal gradient corrected correlation potential by Perdew and Wang [19–21]. To perform the first-principles DFT-B3PW calculations, we used the CRYSTAL2003 computer code [22]. This code employs Gaussian-type functions (GTF) localized at atoms as the basis for an expansion of the crystalline orbitals. Features of the CRYSTAL2003 code, which are most important for this study, are its ability to calculate the electronic structure of materials within both Hartree–Fock and Kohn–Sham (KS) Hamiltonians. An additional advantage of the CRYSTAL2003 computer code is that it treats isolated two-dimensional (2D) slabs, without an artificial periodicity in the Z direction perpendicular to the surface, as commonly employed in some previous surface-band structure calculations [23,24].

In the present paper, we used the same basis sets for the Ca and F atoms as in our previous study [1]. For the O atom we used the basis set given in the Basis Sets Library [22]. The reciprocal space integration was performed by sampling the Brillouin zone of the unit cell with the $8 \times 8 \times 8$ Pack–Monkhorst net [25].

In order to calculate the OV center, we removed one fluorine atom from a 96-atom supercell and replaced a second fluorine atom with an oxygen atom. For the M center system, we calculated a 96-atom supercell with two of the neighbor fluorine atoms removed. After the fluorine atom is removed or replaced with an oxygen atom, the atomic configuration of the surrounding atoms is re-optimized

via a search of the total energy minimum as a function of the atomic displacements from the regular lattice sites. In order to have an accurate description of the anion vacancy, a basis set has been added at the fluorine vacancy, corresponding to the *ghost* atom. For the *ghost* atom, we used the same basis set as that used for F atoms.

The optical absorption energies we calculated as a difference between occupied and unoccupied one-electron energies. In our calculations, we used periodic boundary conditions. Since we used a very large supercell containing 96 atoms, the interaction between periodically translated defects was negligible.

3. OV centers in CaF_2

3.1. OV centers in CaF_2 bulk

As a starting point of our calculations, we performed, using the supercell containing 96 atoms, the geometry relaxation of the atoms surrounding the OV dipole oriented along the (1 0 0) axis in CaF_2 (see Fig. 1). Firstly, the oxygen impurity atom is strongly displaced by 3.02% of the lattice constant (a_0) towards the vacancy. The four nearest fluorine atoms located in the plane containing oxygen are displaced from the oxygen by 1.69% of a_0. The nearest neighbor fluorine atom located above the oxygen is even stronger displaced by 1.92% a_0 from the oxygen.
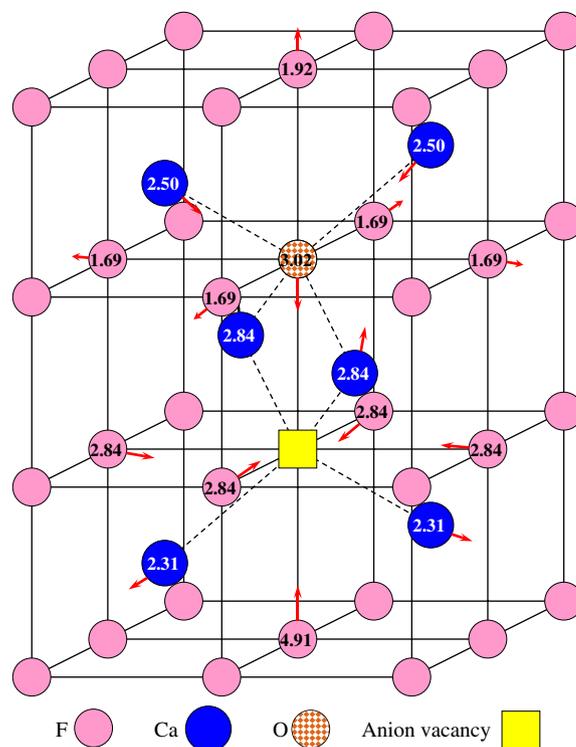

Fig. 1. OV center in CaF_2 oriented along the (1 0 0) axis. The arrows show the directions of the atomic displacements surrounding the OV center, the displacement values are given in circles in % of the lattice constant $a_0 = 5.50$ Å.

The four nearest Ca atoms are strongly attracted by the oxygen impurity atom. So the two Ca atoms located at the plane above the oxygen atom move towards the oxygen impurity by 2.50% of a_0. The two Ca atoms located at the plane below the oxygen atom are even more strongly shifted by 2.84% of a_0 towards the oxygen impurity. According to our calculation, we found that the relaxation of the four Ca atoms surrounding the fluorine vacancy is much stronger than for the F center.

We also calculated the OV dipole oriented along the (110) direction. We found, that the total energy for the (110) case is by 0.32 eV larger than for the (100), i.e., the OV orientation along the (100) direction is energetically more favorable, with respect to the (110) case. Also according to the calculation of Mysovsky et al. [26], the OV dipole (100) orientation is by 0.45 eV more stable as the (110) OV direction. Therefore, we focus our current paper on the investigation of the (100) case.

The charge density map for the OV center in CaF_2 bulk calculated by means of the hybrid B3PW method is shown in Fig. 2. The analysis of the effective charges of OV center and surrounding atoms shows that, unlike the well localized F center in CaF_2, only $-0.082e$ is localized inside the fluorine vacancy. As mentioned before, the stronger relaxation of the four Ca atoms surrounding the fluorine vacancy also can be explained by the delocalized nature of the electron centered at the anion vacancy. The effective charge of the impurity oxygen atom, which replaces the fluorine at the regular crystal site is $-1.598e$ and far from the ideal ionic value of $-2e$. The effective charges ($+1.809e$) of the two Ca atoms located above the oxygen impurity atom are by $0.006e$ lager than in the perfect CaF_2 bulk ($+1.803e$). For the Ca atoms located between the oxygen impurity and the fluorine vacancy, and below the fluorine vacancy, their effective charges are $+1.775e$ and $+1.769e$, respectively. Both values are smaller than in the perfect CaF_2 bulk. The effective charge ($-0.908e$) of
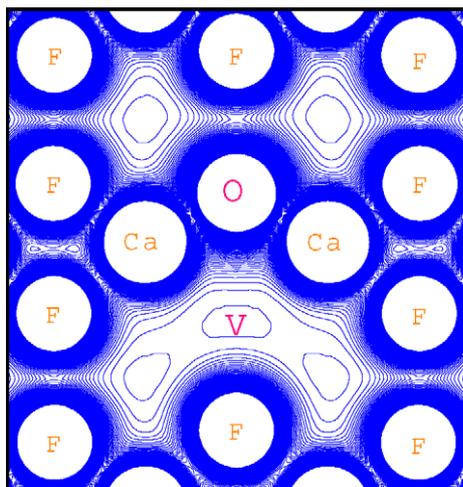
the apical fluorine atom located above the oxygen impurity is by $0.006e$ less than in the CaF_2 bulk ($-0.902e$). The effective charges of the four fluorine atoms located at the same plane as oxygen ion are $-0.901e$. The effective charges of the four fluorine atoms located at the same plane as fluorine vacancy are $-0.905e$. Finally the effective charge of the fluorine atom located below the fluorine vacancy is $-0.897e$ and increases by $0.005e$ in comparison with the CaF_2 bulk. The total charge of the OV center, estimated as a sum of the O and V charges, equals to $-1.680e$, smaller than double of the F charge in the perfect CaF_2 bulk. Thereby, part of the charges of the OV dipole diffuse to the surrounding atoms. Bond population analysis shows that the bond population between the oxygen impurity atom and the fluorine vacancy ($+62me$) is strongly increased with respect to the bond population between two neighbor fluorine atoms ($-22me$) in the perfect CaF_2 crystal.

As a next step we calculated the band structure of the OV center oriented along the (100) axis in CaF_2. The optical band gap between conduction bands (CB) and valence bands (VB) for the CaF_2 containing oxygen impurity atom and fluorine vacancy at the Γ point is 10.79 eV (see Table 1), which is slightly reduced with respect to the optical band gap of the perfect CaF_2 crystal (10.96 eV). The empty defect level induced by the fluorine vacancy, and consisting mainly of s orbitals of the vacancy is located 1.31 eV below the bottom of CB at the Γ point (see Fig. 3). The three

Table 1
Direct optical gaps ($\Gamma \rightarrow \Gamma$) of the OV center in the CaF_2 bulk

Optical gaps	$\Gamma \rightarrow \Gamma$ (eV)
$O_1 \rightarrow V$	6.40
$O_2 \rightarrow V$	6.52
$O_3 \rightarrow V$	6.66
$VB \rightarrow V$	9.48
$O_1 \rightarrow CB$	7.71
$VB \rightarrow CB$	10.79

V indicates the vacancy band; O_1, O_2 and O_3 are three oxygen bands.

Fig. 2. Charge density map of a CaF_2 crystal with the periodic OV center from the (110) side view. Isodensity curves are drawn from $0e$/bohr³ to $0.1e$/bohr³ with an increment of $0.001e$/bohr³.
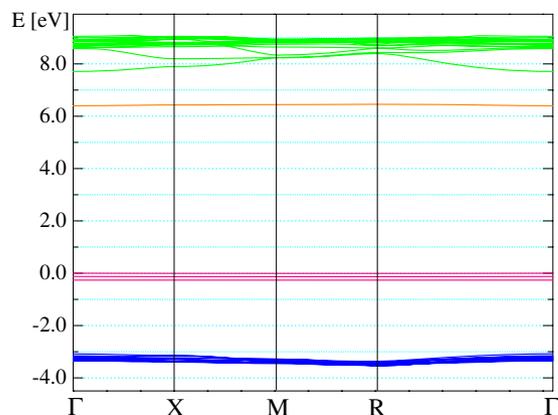

Fig. 3. Calculated band structure for the 96-atom supercell modeling the OV center in CaF_2 bulk.
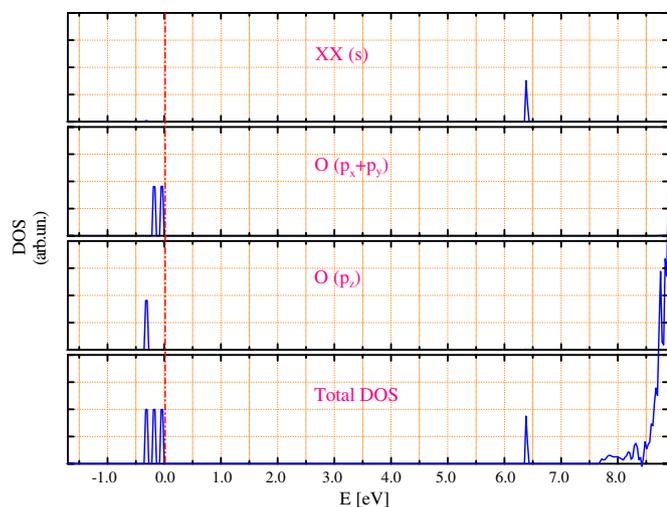
Fig. 4. Density of states (DOS) of the OV center in CaF$_2$ bulk.

Fig. 5. Configurations of aggregation of the OV dipoles in CaF$_2$ bulk.

Table 2
Energies of three different (OV)$_2$-dimer mutual orientations with respect to the configuration 0

Configuration	Our result (eV)	Ref. [26] (eV)
1	+0.54	+0.375
2	+0.37	+0.361
3	+0.34	+0.307

occupied defect levels, induced by the oxygen impurity atom are located 3.08 eV, 2.96 eV and 2.82 eV, respectively, above the VB top at the Γ point. The density of the states (DOS) of the OV center in CaF$_2$ is depicted in Fig. 4. According to the calculated DOS, oxygen p orbitals are split into three bands near the Fermi-energy due to the broken symmetry of the OV center. These three oxygen defect bands near the Fermi-energy are separated by 0.26 eV, which is in the the same energy range as the experimental separation interval of 0.48 eV [26]. Our calculated optical absorption bands above the fluorine vacancy level at the Γ point are 6.40 eV, 6.52 eV and 6.66 eV, respectively, and very close to the complex experimental 6.7 eV absorption bands consisting of at least two elementary peaks with separation of 0.48 eV [27,28]. The calculation of optical absorption bands simply as a difference between occupied and unoccupied one-electron energies which is a very crude approximation, can be justified in our case, since our calculated optical band gap (10.96 eV) is in good agreement with the experiment [1]. The separations of oxygen and vacancy levels induced by the defects in the gap, calculated by Mysovski (5.22 eV, 5.38 eV and 5.61 eV) [26] are in qualitative agreement, but smaller as ours.

Next, we calculated the aggregation of OV dipoles. We considered in our calculations a system which contains two oxygen impurity atoms and two vacancies (see Fig. 5). Configuration 1, 2 and 3 are formed from the configuration 0 when one vacancy switches its position. We found, that the energetically most favorable (OV)$_2$-dimer orientation is configuration 0 (see Fig. 5). The association energy of two dipoles in configuration 0 is 0.55 eV. This energy is the energy difference between the same two remote dipoles and the (OV)$_2$-dimer of configuration 0. So, we can see, that there is some attraction effect between two OV dipoles in a CaF$_2$ crystal. The interaction energy between the periodically repeated OV dipoles in our calculations is negligible. The association energy of two OV dipoles calculated by Mysovski et al. (0.48 eV) [26] is close
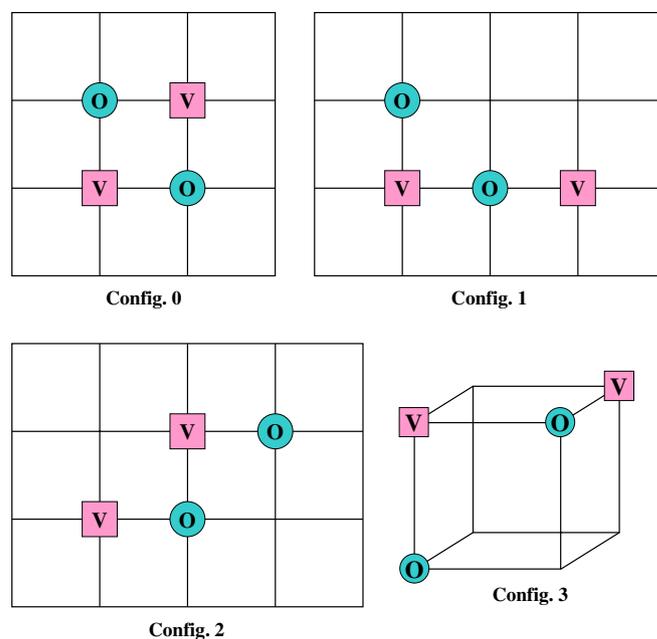
to our result. The relative energies of the configurations 1–3 are given in Table 2.

3.2. OV centers at the CaF$_2$ (111) surface

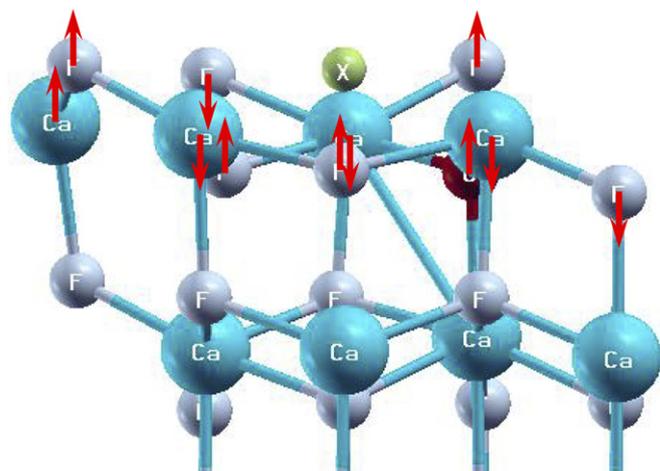We also investigated the OV dipole placed at the CaF$_2$ (111) surface (see Fig. 6), which is the most stable one

Fig. 6. Side view of the OV center placed at the CaF$_2$ (111) surface. The directions of atomic displacements in (111) axis are shown with arrows.
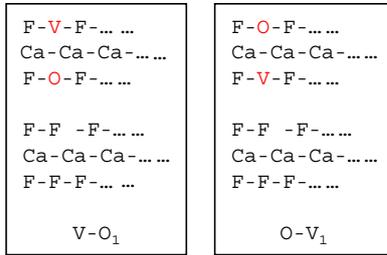
```
F-V-F-… …        F-O-F-… …
Ca-Ca-Ca-… …    Ca-Ca-Ca-… …
F-O-F-… …        F-V-F-… …


F-F -F-… …       F-F -F-… …
Ca-Ca-Ca-… …    Ca-Ca-Ca-… …
F-F-F-… …        F-F-F-… …


   V-O₁              O-V₁
```

Fig. 7. Sketch of the OV center placed at the CaF$_2$ (1 1 1) surface.

among the (1 1 1), (1 1 0) and (1 0 0) terminated surfaces [1]. As we can see in Fig. 7, for the (1 1 1) slab, there are three sublayers in each layer from the side view. For the surface OV center, the oxygen impurity atom and the fluorine vacancy occupy upper and lower fluorine sublayers, respectively. We found, that energetically the most favorable situation for the surface OV center is the situation V–O$_1$ (see Fig. 7). The situation O–V$_1$ is energetically 0.42 eV less favorable, and finally the OV dipole in CaF$_2$ bulk is less energetically favorable, as the surface configuration V–O$_1$ by 0.59 eV. So, it implicates a trend of OV dipoles to locate near the surface.

We also calculated the relaxation of the atoms near the (1 1 1) surface. According to our calculations, the distance between the fluorine vacancy and the oxygen impurity for the V–O$_1$ case is reduced by 0.046 Å (0.84% of a_0) with respect to the bulk OV center case. For the O–V$_1$ case, the O–V distance decreases by 0.159 Å (2.89% of a_0). The effective charges of the OV center at the CaF$_2$ (1 1 1) surface for the V–O$_1$ case are $-0.061e$ for the vacancy and $-1.608e$ for the oxygen impurity. To compare with the OV centers in CaF$_2$ bulk (V: $-0.082e$; O: $-1.598e$), the vacancy charge increases by 0.021e, and the O charge decreases by 0.010e. Unlike the V–O$_1$ case, for the O–V$_1$ case in comparison with OV centers in CaF$_2$ bulk, the oxygen impurity charge ($-1.545e$) increases by 0.053e, and the vacancy charge ($-0.088e$) is reduced by 0.006e. The bond population between the fluorine vacancy and oxygen impurity in the CaF$_2$ (1 1 1) surface is $+52me$ for the V–O$_1$, which is comparable, but slightly weaker, as the corresponding bond population value in CaF$_2$ bulk ($+62me$). However, for the situation O–V$_1$, this bond population ($+70me$) increases slightly by 8me. According to our calculations of OV centers in deeper CaF$_2$ (1 1 1) layers, the differences such as O–V distance, effective charges and bond populations between V–O and O–V configurations become smaller and smaller, and finally disappear.

We also calculated the band structure for the OV center located at the CaF$_2$ (1 1 1) surface (see Fig. 8). The optical band gap between CB and VB ($\Gamma \rightarrow \Gamma$) for the V–O$_1$ system (10.66 eV) is reduced with respect to the CaF$_2$ bulk OV center case (10.79 eV). The narrowing of the surface band gap was observed by us also for ABO$_3$ perovskites [29,30]. The fluorine vacancy induces an empty vacancy level, which consists of the vacancy s orbitals, 0.82 eV below the CB in the V–O$_1$ case. The oxygen p orbitals in
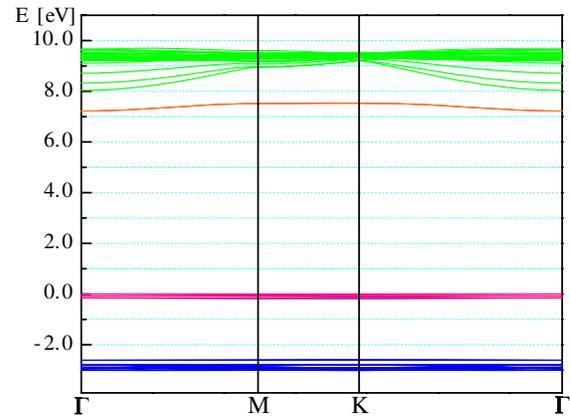

Fig. 8. Band structure of OV center at CaF$_2$ (1 1 1) surface for the V–O$_1$ case.

Table 3
Direct optical gaps (eV) ($\Gamma \rightarrow \Gamma$) of the OV center at the CaF$_2$ (1 1 1) surface

Optical gaps	V–O$_1$	O–V$_1$	Bulk
O$_1 \rightarrow$ V	7.22	6.06	6.40
O$_2 \rightarrow$ V	7.30	6.49	6.52
O$_3 \rightarrow$ V	7.38	6.54	6.66
VB $\rightarrow$ V	9.84	9.82	9.48
O$_1 \rightarrow$ CB	8.04	6.60	7.71
VB $\rightarrow$ CB	10.66	10.36	10.79

V indicates the vacancy band; O$_1$, O$_2$ and O$_3$ are three oxygen bands.

the V–O$_1$ case are split into three bands near the Fermi-energy. The splits are around 0.08 eV, and the separation between oxygen bands O$_1$ and O$_3$ are 0.16 eV. The three oxygen bands in the V–O$_1$ case at Γ point are located 2.62 eV, 2.70 eV and 2.78 eV above the top of VB. In the case of O–V$_1$, the band gap between CB and VB (10.36 eV) is even more strongly reduced with respect to the CaF$_2$ bulk OV center case (see Table 3).

4. M centers in CaF$_2$

F centers in additively-colored alkaline earth fluoride crystals readily aggregate forming more complex centers [31]. The simplest aggregate, the M center (see Fig. 9), is composed of two F centers. We computed a 96-atom super-cell with two of the neighbor fluorine atoms removed.

We calculated the redistribution of the electrons after M center formation. The effective charges of the anion vacancies in the M center case are $-0.759e$ and decrease slightly by 0.007e in comparison with the F-center case ($-0.752e$) [1]. The charge value and charge-density map (see Fig. 10) of the M center show that in CaF$_2$ the charges are well localized inside the M center. Bond population analysis between vacancy–vacancy ($+274me$) in the M center system and F–F bond population ($-22me$) in the perfect CaF$_2$ bulk shows that the major effect observed here is a considerable increase of the chemical bonding covalency.
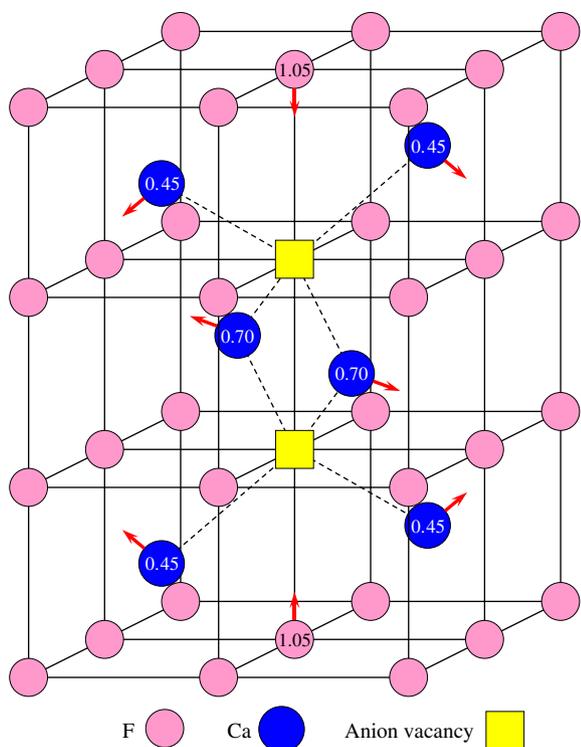
Fig. 9. A view of the M center nearest-neighbor geometry in CaF$_2$ with indication of relaxation shifts. The positions of the anion vacancies are indicated by two squares. The directions of atomic displacements shown with arrows, the values are given in % of the lattice constant.

The displacement values of six Ca atoms surrounding the M center after the lattice relaxation to the minimum of the total energy are given in Fig. 9. The conclusion is that the six neighbor Ca atoms are slightly shifted outwards. According to our calculations, the relaxations of other atoms surrounding the M center are also small and the displacements are all less than 1% of a_0. These slight relaxations of atoms near the M center in CaF$_2$ can be

explained by the fact that the M center charge in CaF$_2$ is close to the double of fluorine charge in CaF$_2$ bulk.

According to our previous research dealing with F centers in CaF$_2$, because of the unpaired electron in single F centers, the band structure of the F-center system is polarized and is separated into two spin band structures, namely α (up-spin) spin structure and β (down-spin) spin structure. The bound unpaired electron level lies in the gap; the corresponding electron–hole level appears in the β spin structure, again in the gap but at positive energies. Unlike unpolarized band structure curves whose one state can be occupied by two electrons, only one electron occupies one state in the polarized band structure. In the ground state, the defect band in the α spin structure is occupied and is unoccupied in the β spin band. The optical absorption corresponds to an electron transition from the F-center ground state to the conduction band. Because of the spin difference between α and β states and the selection
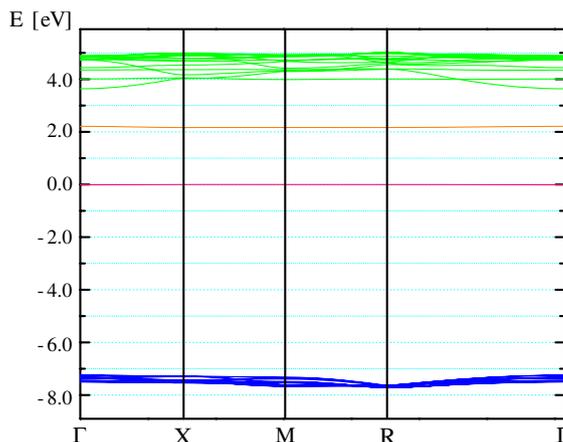

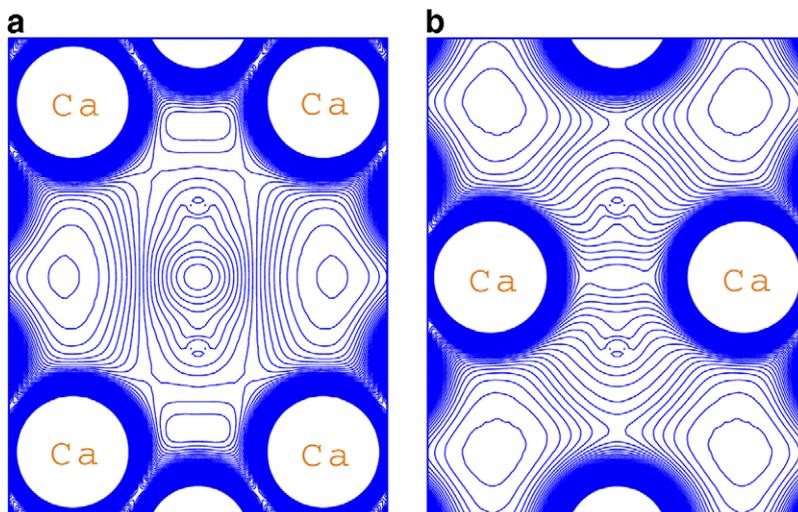Fig. 11. Calculated band structure for the 96-atom supercell modeling the M centers in CaF$_2$.

Fig. 10. Charge density map of a CaF$_2$ crystal with the periodic M center from the $(1\,1\,0)$ (left) and $(1\,-1\,0)$ (right) side view. Isodensity curves are drawn from $0e/\text{bohr}^3$ to $0.1e/\text{bohr}^3$ with an increment of $0.001e/\text{bohr}^3$.

rules, the electron transition from the α occupied band to the β unoccupied band is impossible. The β band absorption is predominantly due to the presence of M centers [31]. In the M center case, the α band can be occupied by two electrons due to unpolarized band structure, so the electron transition from α band to β band is possible. M centers contribute to absorption in the β band and this band will sometimes be referred to as the M band. Our calculation of the direct optical gap ($\Gamma \rightarrow \Gamma$) for M centers in CaF_2 is 2.22 eV (see Fig. 11) and is much smaller than the corresponding value in the F-center case (4.24 eV). The similar phenomenon, decrease of the optical gap for M centers, was also observed for BaF_2 and SrF_2 [31]. Experimentally, the β band is located 2.38 eV above the α band [31]. It means that our calculated result is in good agreement with the experiment.

5. Conclusions

According to our calculated results for the OV centers in CaF_2 bulk, the optical absorption bands at the Γ point are 6.40 eV, 6.52 eV and 6.66 eV, in good agreement with the experimental value (6.7 eV) for the complex absorption band with separation interval of 0.48 eV. Several configurations of the $(OV)_2$-dimer were calculated. The association energy for the most favorable one is 0.55 eV.

The β band absorption in CaF_2 is predominantly due to the presence of M centers. According to our calculations, the direct optical gap ($\Gamma \rightarrow \Gamma$) for M centers in CaF_2 is 2.22 eV, which is in good agreement with the experimental value of 2.38 eV, and much smaller than the corresponding value in the F-center case.

References

[1] H. Shi, R.I. Eglitis, G. Borstel, Phys. Rev. B 72 (2005) 045109.
[2] K. Schmalzl, D. Strauch, H. Schober, Phys. Rev. B 68 (2003) 144301.
[3] N.H. de Leeuw, T.G. Cooper, J. Mater. Chem. 13 (2003) 93.
[4] N.H. de Leeuw, J.A. Purton, S.C. Parker, G.W. Watson, G. Kresse, Surf. Sci. 452 (2000) 9.
[5] M. Verstraete, X. Gonze, Phys. Rev. B 68 (2003) 195123.
[6] G.W. Rubloff, Phys. Rev. B 5 (1972) 662.
[7] J. Barth, R.L. Johnson, M. Cardona, D. Fuchs, A.M. Bradshaw, Phys. Rev. B 41 (1990) R3291.
[8] F. Gan, Y.N. Xu, M.Z. Huang, W.Y. Ching, J.G. Harrison, Phy. Rev. 45 (1992) 8248.
[9] W.Y. Ching, F. Gan, M.Z. Huang, Phy. Rev. B 52 (1995) 1596.
[10] M. Catti, R. Dovesi, A. Pavese, V.R. Saunders, J. Phys.: Condens. Matter 3 (1991) 4151.
[11] A.S. Foster, C. Barth, A.L. Shluger, R.M. Neiminen, M. Reichling, Phys. Rev. B 66 (2002) 235417.
[12] A. Jockisch, U. Schröder, F.W. Wette, W. Kress, J. Phys.: Condens. Matter 5 (1993) 5401.
[13] V.E. Puchin, A.V. Puchina, M. Huisinga, M. Reichling, J. Phys.: Condens. Matter 13 (2001) 2081.
[14] M. Merawa, M. Lunell, R. Orlando, M. Gelize-Duvignau, R. Dovesi, Chem. Phys. Lett. 368 (2003) 7.
[15] A.V. Puchina, V.E. Puchin, E.A. Kotomin, M. Reichling, Solid State Commun. 106 (1998) 285.
[16] W. Hayes, J.W. Twidell, Proc. Phys. Soc. London 79 (1962) 1295.
[17] J. Arends, Phys. Status Solidi 7 (1964) 805.
[18] A.D. Becke, J. Chem. Phys. 98 (1993) 5648.
[19] J.P. Perdew, Y. Wang, Phys. Rev. B 33 (1986) 8800.
[20] J.P. Perdew, Y. Wang, Phys. Rev. B 40 (1989) 3399.
[21] J.P. Perdew, Y. Wang, Phys. Rev. B 45 (1992) 13244.
[22] V.R. Saunders, R. Dovesi, C. Roetti, M. Causa, N.M. Harrison, R. Orlando, C.M. Zicovich-Wilson, CRYSTAL-2003 User Manual, University of Torino, Italy, 2003.
[23] J. Padilla, D. Vanderbilt, Surf. Sci. 418 (1998) 64.
[24] C. Cheng, K. Kunc, M.H. Lee, Phys. Rev. B 62 (2000) 10409.
[25] H.J. Monkhorst, J.D. Pack, Phys. Rev. B 13 (1976) 5188.
[26] A.S. Mysovsky, E.A. Radzhabov, M. Reichling, A.L. Shluger, P.V. Sushko, Phys. Status Solidi (c) 2 (2005) 392.
[27] V.A. Archangelskaya, V.M. Reyterov, L.M. Trofimova, Zh. Prikl. Spektroskopii 32 (1980) 103.
[28] E. Radzhabov, P. Figura, Phys. Status Solidi (b) 136 (1986) K55.
[29] R.I. Eglitis, S. Piskunov, E. Heifets, E.A. Kotomin, G. Borstel, Ceram. Int. 30 (2004) 1989.
[30] E. Heifets, R.I. Eglitis, E.A. Kotomin, J. Maier, G. Borstel, Phys. Rev. B 64 (2001) 235417.
[31] W. Hayes, Crystals with the Fluorite Structure, Clarendon Press, Oxford, 1974.